


Copper complex with sulfamethazine and 2,2'-bipyridine supported on mesoporous silica microspheres improves its antitumor action toward human osteosarcoma cells: cyto- and genotoxic effects

Juan Fernando Cadavid-Vargas · Pablo Maximiliano Arnal · Ruth Dary Mojica Sepúlveda · Andrea Rizzo · Delia Beatriz Soria · Ana Laura Di Virgilio 

Received: 9 May 2018 / Accepted: 9 October 2018 / Published online: 17 October 2018
© Springer Nature B.V. 2018

Abstract Ideal drugs to cure cancer leave normal cells unharmed while selectively turning tumor cells unviable. Several copper complexes have been able to selectively slow down tumor proliferation. We hypothesized that $\text{Cu}(\text{smz})_2(\text{bipy})\cdot\text{H}_2\text{O}$ (**1**)—a copper-complex that has two ligands capable of interacting with DNA—would outperform $\text{Cu}(\text{smz})_2(\text{OH})_2\cdot 2\text{H}_2\text{O}$ (**2**), and also that supporting **1** on mesoporous silica spheres would decrease even further tumor cell viability in vitro. After exposing osteosarcoma cells (MG-63) and normal phenotype cells of bone origin (MC3T3-E1) to either complex, we studied their toxic effect and mechanisms of

action. We determined cell viability (MTT assay) and quantified formation of reactive oxygen species (oxidation of DHR-123 to rhodamine). Moreover, we assessed genotoxicity from (i) formation of micronucleus (MN assay) and (ii) damage of DNA (Comet assay). After the exposure of **1** supported on silica spheres, we tested cell viability. Our results confirm our hypotheses: inhibition of tumor cells follows: supported **1** > dissolved **1** > **2**. Future work that enhances the load of the complex exclusively in mesopores may improve the ability of **1** to further inhibit tumor cell viability.

Keywords Antitumor effect · Copper(II) complexes · Cytotoxicity · Genotoxicity · Mesoporous silica microspheres

Electronic supplementary material The online version of this article (<https://doi.org/10.1007/s10534-018-0154-y>) contains supplementary material, which is available to authorized users.

J. F. Cadavid-Vargas · R. D. Mojica Sepúlveda · A. Rizzo · D. B. Soria · A. L. Di Virgilio (✉)
CEQUINOR (CONICET-UNLP), Facultad de Ciencias Exactas, Universidad Nacional de La Plata, 47 y 115, 1900 La Plata, Argentina
e-mail: aldivirgilio@biol.unlp.edu.ar

P. M. Arnal
CETMIC (Centro de Tecnología de Recursos Minerales y Cerámica), Cno Centenario y 506, CC 49, B1897ZCA M.B. Gonnet, Buenos Aires, Argentina

P. M. Arnal · A. L. Di Virgilio
Facultad de Ciencias Exactas, Universidad Nacional de La Plata, 47 y 115, 1900 La Plata, Argentina

Introduction

One strategy used to develop new drugs that inhibit tumor proliferation rest on the ability of some copper complexes to selectively interfere with the mechanism of cellular division in tumor cells (Boulsourani et al. 2017; León et al. 2016; Oliveri et al. 2017). Some copper complexes selectively damage DNA in such way that cell cannot repair DNA after mitosis. Copper complexes bind to DNA (Buchtík et al. 2011; Galindo-Murillo et al. 2011) and trigger redox-reactions that

can damage and even cleave strands. Being unable to cross the G2/M checkpoint, damaged cells progressed to early apoptosis (Chen et al. 2010; Ferrari et al. 2004; Zhang et al. 2007) and to cell death (Arjmand and Muddassir 2011; Buchtík et al. 2012; Chen et al. 2010). Other copper complexes disable an enzyme that participate in the replication and transcription of DNA (topoisomerase) and create transient DNA breakages (Duff et al. 2012; Seng et al. 2012).

Sulfamethazine (smz) and 2,2'-bipyridine (bipy) can both bind to metal ions and interfere with DNA. Both smz (Hossain et al. 2007; Gutiérrez et al. 2001; Öztürk et al. 2015; Tommasino et al. 2011) and bipy (Lobana et al. 2014; Piotrowska-Kirschling et al. 2018) bind to metallic ions to form water soluble complexes. Furthermore, smz is a sulfa-based drug reported as antibacterial agent that prevents DNA replication (Anderson et al. 2012), and bipy interacts with DNA either by electrostatic interaction (Carter et al. 1989) or by intercalation (Cusumano et al. 2005). However, the ability of complexes of copper with smz and bipy to inhibit proliferation of tumors remains unknown.

In this work, we asked whether $\text{Cu}(\text{smz})_2(\text{bipy})\cdot\text{H}_2\text{O}$ (**1**) outperform $\text{Cu}(\text{smz})_2(\text{OH})_2\cdot 2\text{H}_2\text{O}$ (**2**) as inhibitor of tumor cell viability, and whether the complex supported on mesoporous silica spheres—a promising drug delivery system (Mai et al. 2017; Wang et al. 2016; Xu et al. 2016) able to cross cell walls with its cargo—outperform dissolved complexes. We first determined viability (MTT assay) of non-tumor cells (MC3T3-E1) and tumor cells (MG-63) of bone origin exposed to either **1** or **2**. These two cell lines are generally used to assess the effects of biomaterials on cell behavior. In fact, MC3T3-E1 cells -that has similar growth rate of human osteoblast cells- are suitable for the evaluation of biomaterials and represent a reliable alternative to the primary human osteoblast in vitro cell model for various research areas (Czekanska et al. 2012). Moreover, human osteosarcoma cell line MG-63 is one of the most employed cell line to study bone tumors on account of its molecular composition of the osteosarcoma extracellular matrix (Pautke et al. 2004). After exposing cells to either complex, we quantified formation of reactive oxygen species (ROS). Moreover, we assessed genotoxicity of **1** from (i) formation of micronucleus (MN assay) and (ii) damage of DNA (Comet assay). Additionally, we checked endocytosis

of mesoporous, silica spheres by transmission electron microscopy (TEM) and determined cell viability after exposure to **1** supported on mesoporous, silica spheres. The results of this research work not only fill the knowledge gap of how **1** and **2** exert a cyto- and genotoxic effects, but also hint in which direction future work on the development of drugs that inhibit tumors may proceed.

Experimental

Materials

Tissue culture materials were purchased from Trading New Technologies (Buenos Aires, Argentina). Dulbecco's modified Eagles medium (DMEM), fetal bovine serum (FBS) from GBO Argentina SA (Buenos Aires, Argentina); TrypLE™ was provided by Gibco (Gaithersburg, MD, USA). Cytochalasin B from *Dreschlera dematioides*, 3(4,5-dimethylthiazol-2-yl)-2,5-diphenyltetrazolium bromide (MTT), Trypan Blue, hexadecylamine and TEOS were obtained from Sigma Chemical Co. (St. Louis, Mo, USA). Dihydrochlorodamine 123 (DHR) was from Molecular Probes (Eugene, OR, USA). Bleomycin (BLM) (Bleomycin®) was kindly provided by Gador S.A. (Buenos Aires, Argentina). Syber Green and low-melting-point agarose were purchased from Invitrogen Corporation (Buenos Aires, Argentina).

Synthesis and physicochemical characterization of copper coordination complexes

1 and **2** were synthesized as previously described (Mansour and Mohamed 2015; Tommasino et al. 2011). Briefly, **2** was prepared by dissolving 2 mmol of sodium sulfamethazine with 1 mmol of $\text{CuSO}_4\cdot 5\text{H}_2\text{O}$ in 20 mL water and the solution was heating to reflux for 2 h, where a brick-red complex was isolated, separated by filtration and washed with water. **1** was synthesized by adding 1 mmol of 2,2'-bipyridine to 1 mmol aqueous solution of $\text{CuSO}_4\cdot 5\text{H}_2\text{O}$, and the solution was gently heated until complete dissolution of the secondary ligand, and colour change. Next, an aqueous solution of sodium sulfamethazine (2 mmol) was added and the resulting solution was refluxed for 4 h, where a green complex precipitated.

Synthesis of mesoporous silica spheres

Mesoporous silica microspheres were synthesized according to the literature (Dong et al. 2003). Briefly, hexadecylamine (2.08 g) as mesoporegen, distilled water (180 mL) and 2-propanol (200 mL) as solvents, and $\text{NH}_3\text{-H}_2\text{O}$ (28%, 3.2 mL) as base catalyst were mixed together until a homogeneous solution was formed. TEOS (12 mL) as silica source was added, and the final mixture was stirred for another 1 min before it was aged overnight at room temperature. The product was recovered by filtration and washing with water. To remove organic templates from the pores, the as synthesized material was heated in air at 550 °C for 6 h.

Cell culture and incubations

Human osteosarcoma (MG-63) and mouse calvaria (MC3T3-E1) cell lines were originally purchased from ATCC (CRL1427TM and CRL-2593TM respectively). Cells were grown in Dulbecco's Modified Eagle's Medium (DMEM) containing 10% FBS, 100 U mL⁻¹ penicillin and 100 µg mL⁻¹ streptomycin at 37 °C in a 5% CO₂ atmosphere. Cells were seeded in a 25 cm² flask and when 70–80% of confluence was reached, cells were subcultured using 1 mL of TrypLETM. For experiments, cells were grown in multi-well plates. When cells reached the desired confluence, the monolayers were washed with DMEM and were incubated under different conditions according to the experiments.

Fresh stock solutions of the complexes were prepared in dimethyl sulfoxide at 100 mM and diluted according to the concentrations indicated in the figures. To test the stability of **1** and **2** under the experimental conditions used in this work, we analysed the UV–Visible spectra of different solutions of the complexes. The electronic spectra were recorded at times ranging from 0 to 24 h (see Supplementary Information Fig. 1).

Cell viability

Cell viability was assayed by the MTT assay. The MTT assay was carried out according to (Mosmann 1983). Briefly, after treatments with different concentrations of the complexes or particles, the cells were incubated with 0.5 mg/mL MTT for 3 h. Cells were

lysed in dimethyl sulfoxide. Color development was measured at 570 nm. Results were expressed as the mean of three independent experiments and plotted as percent of control.

In order to determine whether reactive oxygen species provoked cellular death, we added the antioxidant N-acetyl cysteine (NAC) to the cultures exposed to the complexes. Cells at confluence were pretreated with 250 µM NAC for 2 h, after which the medium was replaced with a new one containing different concentrations of the complexes; cytotoxicity was assessed as previously described.

Cell viability was also determined in human osteosarcoma and normal phenotype osteoblast cell lines for supported **1**. It was determined at 1000 µg/mL since it is the concentration used in the dissolution assay (see “[In vitro dissolution of 1 supported on silica spheres](#)” section. *In vitro dissolution study*). Assuming a similar behavior in DMEM, we used the concentrations of **1** (found at 24 h in the *in vitro* dissolution study) to compare the effect of the direct exposure of **1** and its effect when it is released from the particles.

Quantification of reactive oxygen species (ROS) within cells

Intracellular ROS were determined by oxidation of Dihydrorhodamine-123 (DHR-123) to rhodamine by spectrofluorescence. This probe measures levels of ROS intermediates such as peroxyne, H₂O₂ and the hydroxyl radical OH. (Royall and Ischiropoulos 1993). Briefly, MG-63 cells were incubated at 37 °C with different concentrations of the complexes. After 24 h, cells were incubated with 10 mM DHR-123. After 1 h, cells were scraped into 1 mL 0.1% Triton-X100. The cell extracts were then analyzed for the oxidized product rhodamine by measuring fluorescence (excitation wavelength, 495 nm; emission wavelength, 532 nm), using a Shimadzu Spectrofluorophotometer RF-6000 equipped with a computer working with LabSolutions RF software. Results were corrected for protein content with the PierceTM BCA Protein Assay Kit.

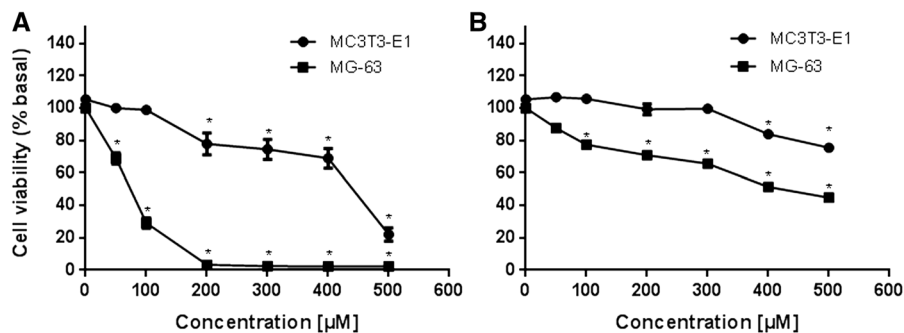


Fig. 1 Effects of **1** (a) and **2** (b) on MG-63 and MC3T3-E1 cell viability. Cells were incubated alone (control) or with different concentrations of the compounds at 37 °C for 24 h. The results are expressed as the percentage of the basal level and represent

the mean \pm the standard error of the mean (SEM) ($n = 12$). Asterisks represent a statistically significant difference in comparison with the basal level (MG-63 $p < 0.001$ and MC3T3-E1 $p < 0.01$)

Quantification of micronucleus with Cytokinesis-block micronucleus (CBMN) assay

The CBMN assay is used in toxicology to screen potentially genotoxic compounds. Micronuclei are cytoplasmic bodies that have a portion of the acentric chromosome or the whole chromosome which were not carried during the anaphase, thus resulting in the absence of whole chromosomes or parts of them from the main nuclei. Experiments were set up with cultures in the log phase of growth. MG-63 cells were treated with different concentrations of **1** along with cytochalasin B (4.5 µg/mL). After 24 h, cells were rinsed and subjected to hypotonic conditions, fixed with methanol at -20 °C and stained with 5% Giemsa. For the analysis, 500 binucleated (BN) cells were scored at $\times 400$ magnification per experimental point from each experiment. The examination criteria employed were reported by Fenech (2000).

Quantification of DNA damage with single cell gel electrophoresis (Comet) assay

For detection of DNA damage, the Comet assay was employed based on the method of Singh et al. (1988), with minor modifications. Briefly, MG-63 cells were treated with different concentrations of **1**. After 24 h, cells were suspended in 0.5% low melting point agarose and immediately poured onto microscope slides precoated with 0.5% normal melting point agarose. Two slides were prepared for each condition; one slide was used to observe single-strand DNA breaks and the other, in order to obtain information on the presence of oxidized DNA bases using a digestion

with the enzyme EndoIII (Azqueta and Collins 2013). Slides were immersed in ice-cold lysis solution (2.5 M NaCl, 100 mM Na₂-EDTA, 10 mM Trizma-HCl, pH 10 and 1% Triton X-100, 10% dimethyl sulfoxide at 4 °C, pH 10) for 1 h in order to lyse the cells, remove cellular proteins and to permit DNA unfolding. After that, the slides were washed three times (5 min each time) with enzyme buffer (0.1 M KCl, 0.5 mM Na₂-EDTA, 40 mM HEPES-KOH, 0.2 mg/ml BSA, pH 8.0) and incubated for 45 min at 37 °C with EndoIII in the enzyme buffer or with buffer alone. The slides then were placed on a horizontal gel electrophoresis tank and the DNA was allowed to unwind for 20 min in freshly prepared alkaline electrophoresis buffer (300 mM NaOH and 1 mM Na₂-EDTA, pH 12.7). Electrophoresis was carried out in the same buffer for 30 min at 25 V (≈ 0.8 V/cm across the gels and ≈ 300 mA) in an ice bath condition. Afterwards, slides were neutralized and stained with SyberGreen. Analysis was performed in an Olympus BX50 fluorescence microscope. A total of 100 randomly captured cells per experimental point were used to determine the tail moment using Comet Score version 1.5 software.

Uptake and subcellular localization of silica microspheres by TEM

After treatment with 50 µg/mL of silica particles, MG-63 cells were fixed in 2% glutaraldehyde for 1 h at 4 °C. Later, cells were treated with 2% OsO₄ in sodium cacodylate and embedded in epoxy resin, Epon (Serva, Heidelberg, Germany). Ultrathin sections (60 nm) were obtained by ultramicrotome (Supernova Reichert-J). These sections were stained with

uranyl acetate solution in acetic acid and plumbic citrate. TEM analyses of ultrathin sections allowed determining the distribution of the particles within the cells, placing the ultrathin sections on 150 mesh grids and examining by a TEM microscope (JEOL JEM 1200 EX II).

Preparation of **1** supported on silica spheres

10 mg of silica microspheres and 2 or 5 mg of **1** (ratio 1:1/5 and 1:1/2, respectively) were stirred in 5 mL distilled water during 48 h. The final concentrations of **1** used to prepare the formulations were 506 and 1264 μM , respectively. Then the powdered products were centrifuged and extensively washed and dried at 37 °C till constant weight.

Characterization of **1** supported on silica spheres

The synthesized materials were characterized by FTIR spectra, thermogravimetric analysis (TGA), Scanning Electronic Microscopy (SEM) and by physical N_2 adsorption. The FTIR spectra were carried out with a Bruker EQUINOX 55 spectrophotometer (Billerica, MA, USA), in the range from 4000 to 400 cm^{-1} using the KBr pellet technique, with a spectral resolution of 4 cm^{-1} . TGA was performed using Shimadzu TGA-50 unit (Kyoto, Japan), at a heating rate of 5 °C min^{-1} and nitrogen flow of 50 mL min^{-1} . Moreover, characterization of the original and the treated silica microspheres was performed by SEM using a Philips SEM 505 combined with semiquantitative analysis by energy dispersive X-ray analysis (EDS) by an analyzer EDAX 9100. Surface areas and porosity of samples were determined by physical N_2 adsorption at 77 K using a Micromeritics apparatus ASAP 2010. Prior to measurement, the material was activated under vacuum at 150 °C for at least 2 h. Specific surface area was calculated using the Brunauer–Emmett–Teller (BET) method.

In vitro dissolution of **1** supported on silica spheres

An in vitro dissolution study was performed in phosphate buffer (pH 7) at 37 °C. Silica spheres supporting **1** (5 mg) were incubated in 5 mL phosphate buffer at 37 °C (1000 $\mu\text{g/mL}$). At appropriate time intervals, samples were withdrawn from the medium and analyzed by UV–Vis spectroscopy at a

wavelength of 240 nm. The concentration of the dissolved **1** was calculated according to a calibration curve ($y = 38966.24x + 0.0221$, $R^2 = 0.9999$). The UV–Vis spectra were recorded employing a Shimadzu UV-2600 Spectrophotometer (Kyoto, Japan).

Statistical analysis

Results are expressed as the mean of three independent experiments and plotted as mean \pm standard error of the mean (SEM). The total number of repeats (n) is specified in the legends of the figures. Statistical analysis of the data was carried out by ANOVA, followed by the Fisher's Least Significant Difference (LSD) procedure to discriminate among the means. The statistical analyses were performed using STAT-GRAPHICS Centurion XVI.I. In the comet assay, Mann–Whitney Rank Sum Test was carried out to compare treated cells group against the control group and against each other.

Results

Effect of copper complexes on cell viability

Osteosarcoma cells (MG-63) became totally unviable when exposed to 200 μM of **1** (Fig. 1a) but kept 70% viability when exposed to 200 μM of **2** (Fig. 1b) ($p < 0.001$). Half maximal inhibitory concentrations (IC_{50}) also show that **1** ($\text{IC}_{50} = 62 \mu\text{M}$) outperformed **2** ($\text{IC}_{50} = 472 \mu\text{M}$) in inhibiting cell viability of tumor cells. It is worth mentioning that **2** only reduced 50% tumor cell viability at the highest tested concentration (500 μM , Fig. 1b).

Normal phenotype osteoblasts (MC3T3-E1) experienced a significant reduction of viability when exposed to 200 μM of **1** and 400 μM of **2** ($p < 0.01$). Thus, an exposure of cells to **1** with a concentration between 100 and 200 μM may offer optimal conditions to reduce tumor cell without affecting normal cells.

The complex **1** also outperformed its constituents— $[\text{Cu}(\text{H}_2\text{O})_6]^{2+}$, smz, and bipy—in decreasing the viability of tumor cells (Fig. 2). When we watch the effect of exposing tumor cells to 200 μM of either constituent, we see that bipy reduced viability to 80%, $[\text{Cu}(\text{H}_2\text{O})_6]^{2+}$ reduced viability to 85%, and smz did not significantly reduce viability at all. This finding

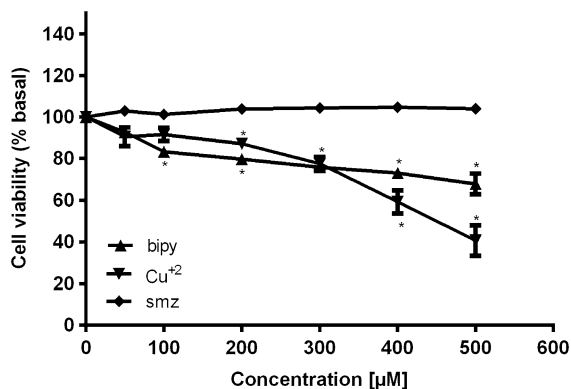


Fig. 2 Effects of bipy, smz and Cu²⁺ on MG-63 human osteosarcoma cell viability. Cells were incubated alone (control) or with different concentrations of either compound at 37 °C for 24 h. The results are expressed as the percentage of the basal level and represent the mean ± the standard error of the mean (SEM) (n = 12). Asterisks represent a statistically significant difference in comparison with the basal level (p < 0.001)

strongly contrasts with what we mentioned above that 200 µM of **1** turned osteosarcoma cells nonviable.

Effect of copper complexes on oxidative stress

The significant reduction in viability of tumor cells when exposed to **1** within the concentration range 50 to 100 µM occurred while a significant concentration of ROS formed within cells (p < 0.001) (Fig. 3). The inability of **2** to significantly reduce tumor cell viability at 50 µM and the ability of **2** to significantly

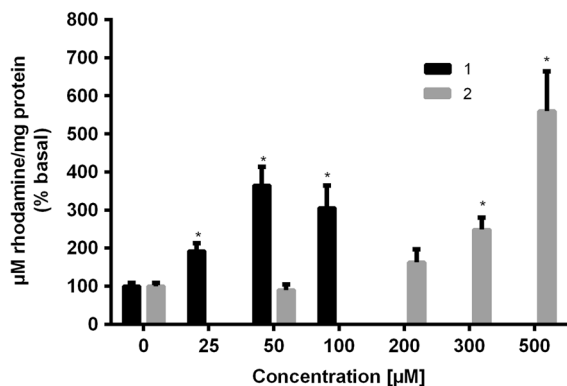


Fig. 3 **1** and **2** induced formation of reactive oxygen species (ROS) in MG-63 cell line. ROS production in the cells was evaluated through the oxidation of dihydrorhodamine 123 (DHR-123) to rhodamine123. The results are expressed as the mean ± SEM (n = 10). Asterisks represent a statistically significant difference in comparison with the basal level (p < 0.001)

solely reduce about 20% at 100–200 µM occurred without a significant formation of ROS, which only increased at higher concentrations (p < 0.001).

An independent way to determine whether an increase in ROS level is responsible for the reduction in cell viability consists in adding antioxidants before exposing tumor cells to either **1** or **2**. N-acetyl cysteine (NAC) is a well known antioxidant capable of removing ROS. Tumor cells treated with NAC before exposing to **1** (50–200 µM) experienced a partial but significant improvement of cell viability (Fig. 4). Thus, reduction of viability of tumor cells rest at least in part in the formation of ROS. The partial recovery of cell viability suggests that either other mechanisms may be involved or that NAC was unable to cope with the attack of ROS. Tumor cells treated with NAC before exposing to **2** (50–200 µM) experienced no significant improvement of cell viability (Fig. 4). Thus, the significant reduction of cell viability observed after exposure to **2** at 100 and 200 µM (Fig. 1b) may not be attributed to ROS but to different source of damage.

Effect of **1** on cellular nuclei

Tumor cells exposed to low concentrations of **1** experienced a significant increment in micronuclei formation (Fig. 5a). A concentration of 10 µM significantly favored formation of micronuclei and a concentration of 25 µM provoked the same effect of bleomycin (0.7 µM) that we used as a positive control

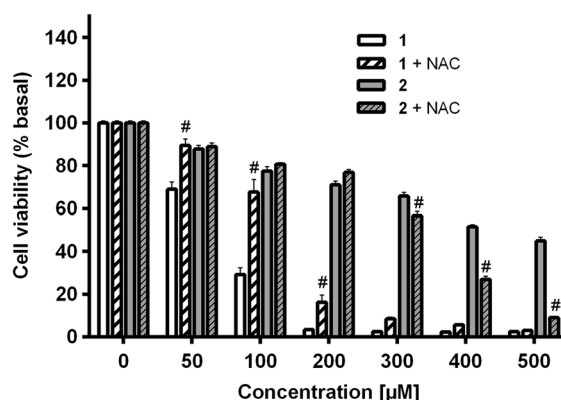


Fig. 4 Influence of the addition of N-acetyl cysteine (NAC) to cell viability of MG-63 in the presence of either **1** or **2**. The results represent the mean ± SEM (n = 18). Asterisks represent a statistically significant difference in comparison with the basal level (p < 0.001). Number sign represent statistically significant differences between treatments (p < 0.01)

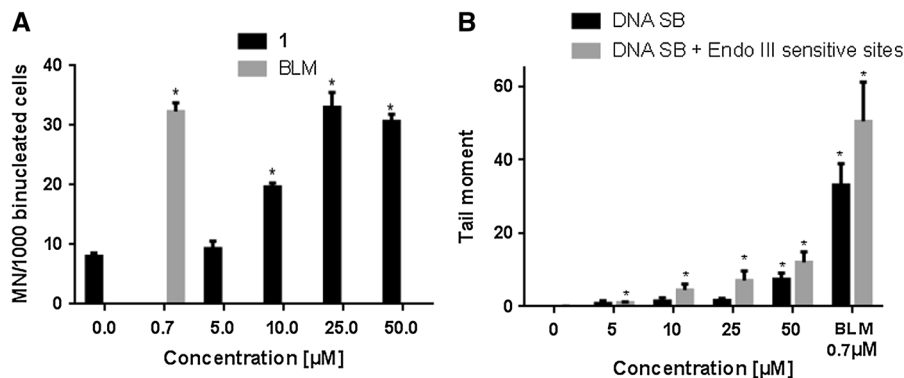


Fig. 5 Genotoxicity of **1** toward MG-63 tumor cells expressed in terms of formation of micronuclei and of breakage of DNA. **a** Micronucleus assay: induction of micronuclei in MG-63 cells after 24 h exposure to **1**. Asterisk represent a statistically significant difference at $p < 0.01$. Bleomycin (BLM) 0.7 μM was used as a positive control. **b** DNA strand breaks and oxidative damage in MG-63 cells after 24 h of incubation with different concentrations of **1** by the Comet assay. Black bars

represent nuclei incubated with the buffer without enzymes (buffer): represent only strand breaks. Grey bars represent nuclei post-digested with EndoIII: represent strand breaks and strand damage (oxidized). The results are expressed as the mean \pm SEM ($n = 150$). Asterisk represent a statistically significant difference at $p < 0.01$. Bleomycin (BLM) 0.7 μM was used as a positive control

($p < 0.01$). Thus, concentrations of **1** that provoked a reduction in cell viability of up to 40% produced a significant genotoxic effect.

Additionally, tumor cells exposed to low concentrations of **1** experienced a significant damage of DNA. A concentration of 5 μM started to significantly damage DNA but a concentration of 50 μM was necessary to significantly break and liberate DNA-strands (Fig. 5b). A significant increase was observed in oxidative DNA damage detected by the employment of EndoIII, for the detection of oxidized pyrimidines in all the concentrations tested ($p < 0.01$). Thus, when oxidative DNA damage was investigated, an increase in DNA strand breaks was observed at lower concentrations.

Preparation and characterization of mesoporous microspheres supported **1**

We saw that **1** outperformed **2** when both were present as part of a solution (hypothesis 1), but we wanted to know if supported **1** on mesoporous silica spheres outperform **1** in solution (hypothesis 2).

First, we verified if mesoporous microspheres with a diameter of ca. 1 μm (see in SI characterization of the material) could cross membranes of tumor cells without causing any detectable harm. Tumor cells exposed to silica spheres in the concentration range 10–1000 $\mu\text{g/mL}$ experienced no significant reduction

in cell viability and neither formed significant concentrations of ROS ($p < 0.05$, data not shown). On the other hand, tumor cells exposed to silica spheres (50 $\mu\text{g/mL}$) for 2 h partially incorporated silica spheres that located exclusively in the cytoplasm and formed pseudopodium-like cytoplasm projections of the cell membrane before endocytosis (Fig. 6).

Second, we supported two different amounts of **1** on mesoporous silica microspheres and characterized the supported complex (See Supplementary Information).

In vitro dissolution of **1**

The kinetic of dissolution of the complex from the two formulations are presented in Fig. 7. The release rate and the amount released were load dependent. Both samples showed a faster initial release followed by a constant release rate, which lasted until the end of the experiment. Most of **1** was released during the first 24 h. At this time, the concentration released increased almost twofold when the loading did ($40.9 \pm 6.8 \mu\text{M}$ and $109.1 \pm 11.8 \mu\text{M}$ for the material prepared from 506 μM and 1264 μM of **1**, respectively).

Effect of supported **1** on cell viability

The study of cell viability showed that supported **1** outperformed dissolved **1** in decreasing viability of

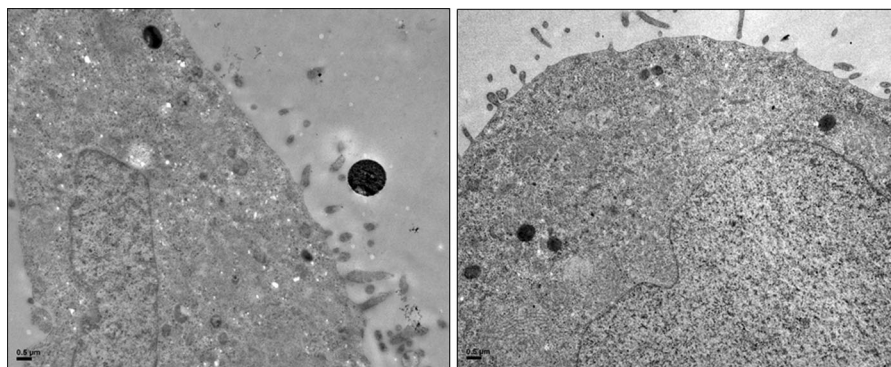


Fig. 6 MG-63 cells incorporated silica spheres after exposure to a dispersion (50 $\mu\text{g}/\text{mL}$) during 24 h (endocytosis). Left transmission-electron-microscopic image shows initial changes in the cell membrane previous to endocytosis, showing

pseudopodium-like cytoplasm projections of the cell membrane. Right transmission-electron-microscopic image shows intracellular phagocytosed material

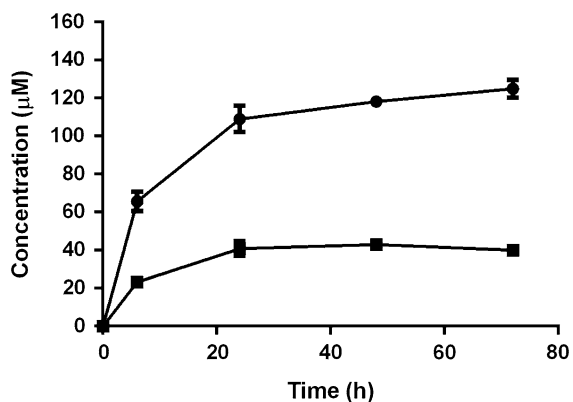


Fig. 7 Kinetic of dissolution of **1** supported on silica spheres. Data are expressed as the mean \pm SEM. Supported materials were prepared with solutions of the complex with two different concentrations: Filled square and filled circle represent materials prepared from solutions having 506 μM and 1264 μM of **1**, respectively

osteosarcoma cells. After an exposure of 24 h, supported **1** produced a significant reduction of cell viability compared to dissolved **1** (Fig. 8) for both concentration tested. On the other hand, the effect of the supported **1** on normal phenotype mouse calvaria cells slightly, but not significantly, increased in comparison to the direct exposure.

Discussion

Silica spheres with mesoporous pores (2–50 nm) are one of the promising drug delivery systems due to its large surface area, tunable pore size distribution, high

pore volume and the capability of being modified by different functional groups (Mai et al. 2017; Wang et al. 2016; Xu et al. 2016). Moreover, it has been shown that they are good carriers for anticancer drugs (Chang et al. 2016; Lu et al. 2007; Martínez-Carmona et al. 2016). However, this aspect has never been investigated with a copper coordinated compound. Here, for the first time, we studied a material made of silica microspheres and a heteroleptic copper(II) compound -which is also studied for assessing its toxic effect and mechanism of action- and resulted to be a promising antitumor agent against human osteosarcoma cells.

1 Outperformed 2 in reducing viability of tumor cells

In the present study, osteosarcoma cell viability was investigated by measuring the alteration in the energetic metabolism of the cells (MTT assay). This technique measures the ability of the mitochondrial succinic dehydrogenases to reduce the methyl tetrazolium salt. Our results probed an improvement of the antitumor action through the complexation with both smz and bipy. Previously, we have also showed that the complexation of Cu(II) with both saccharinate and glutamine improved the antitumor activity in comparison to the homoleptic complexes (Cadavid-Vargas et al. 2017). It has been also shown that the bipy ligand has an important role in the cytotoxic effect. In agreement with our finding, the Cu(II) and 2,2'-bipyridine complexation with naringenin was more

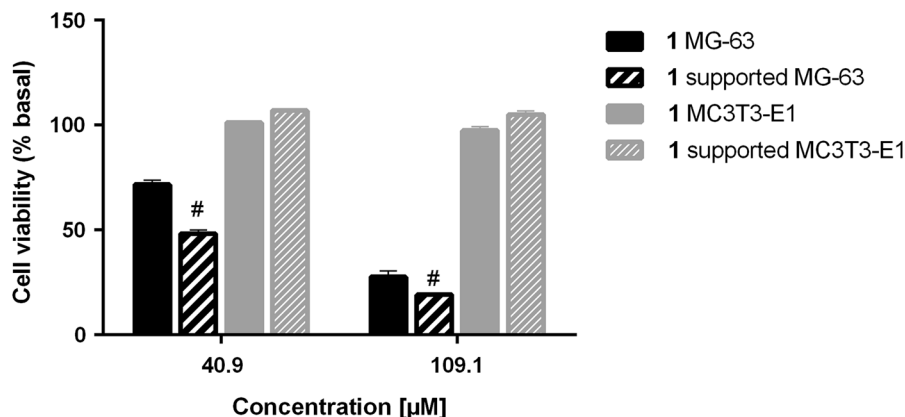


Fig. 8 Effect of **1** supported on silica microspheres in comparison to the direct exposure on MG-63 or MC3T3-E1 cell viability. Cells were incubated alone (control) or with different concentrations of **1** dissolved or supported on

efficient inhibiting colony formation, proliferation and migration of breast tumor cells, than naringenin itself (Filho et al. 2014). Moreover, a nitrate bridged homodinuclear (Cu-Cu) complex containing 2,2'-bipyridine showed a significant cytotoxicity against HeLa cell line in vitro with an IC_{50} value lower than the found here (Gaur et al. 2017). However, **1** still resulted to be a very good candidate for cancer chemotherapy since it keeps cell viability in normal phenotype osteoblasts above 70% up to 400 μ M and is highly deleterious for human osteosarcoma cells.

Formation of ROS underlie the selective attack of **1** to tumor cells

It has been shown that copper complexes induce the formation of ROS that generate harmful effects in cells (Cadavid-Vargas et al. 2017; Karlsson et al. 2017). Cells can cope with the damage caused by ROS up to a certain point from which they may irreparably damage biomolecules and kill cells (Nordberg and Arnér 2001). Our findings indicate that incubation of osteosarcoma cells with copper complexes caused an increase in the production of ROS which has a vital role in cell viability. From 50 to 100 μ M of **1**, a pronounced oxidative stress is generated that translates into a severe damage on cellular viability. The presence of NAC could eliminate intracellular free radicals and ROS which improved cell survival. On the other hand, the failure of **2** to significantly induce the formation of ROS agrees with the inability to

mesoporous spheres (1000 μ g/mL) at 37 °C for 24 h. The two concentrations chosen were those found at 24 h in the in vitro dissolution study. The results are expressed as the percentage of the basal level (n = 12)

reduce the tumor cell viability more than 70% (and to recover cell viability in the presence of NAC) up to 200 μ M. The deleterious effect of **2** from 300 μ M - along with an increase in ROS level- could not be overcome and even increased with a pre-incubation of NAC. It has been shown that NAC can exert pro- and antioxidant effects depending on the intracellular redox environment characterized by GSH/GSSG balance, which could either promote or inhibit cell survival (Finn and Kemp 2012).

Genotoxic effects of **1**

Cell viability can decrease for several reasons being one of them that mitochondrial metabolism fails (as we found with the MTT assay), but it can also decrease when nuclei are damaged. One consequence of damaged nuclei is the formation of micronuclei—cytoplasmic body having either a portion of an acentric chromosome or the whole chromosome (Stopper and Müller 1997), which normally develops a nuclear membrane. Another strategy for studying the genotoxic effects is through the induction of DNA damage by the Comet assay.

Several mechanisms of interaction with DNA have been described for copper compounds, such as phosphate hydrolysis and/or base-pair intercalation (Galindo-Murillo et al. 2015). Besides, it has been reported that copper coordinated compounds induced ROS-mediated genotoxicity in mammalian cells (Santini et al. 2014; Serment-Guerrero et al. 2011). In the

present study, we observed a genotoxic effect caused by **1** that could be explained by the increase in the level of ROS, since at low concentrations a significant increase of oxidized pyrimidines was detected. It has previously been shown that the interaction with DNA of a series of copper complexes—among which there is one with bipyridine as a ligand—triggers the cleavage of the biomolecule by a mechanism of action involving free radicals (Becco et al. 2014).

Supported **1** outperformed dissolved **1** in decreasing viability of tumor cells

Mesoporous silica spheres were employed to support **1**. This material—which it turned out to be non-toxic-internalized and was found exclusively in the cytoplasm. It induced changes in cell membranes previous to endocytosis, showing pseudopodium-like cytoplasm projections. It has been previously demonstrated that mesoporous silica materials are promising delivery systems because their biocompatibility among other chemical properties. Besides, the mechanism of cellular uptake appears to be mediated by an active endocytosis pathway as demonstrated when the process stopped when temperature dropped to 4 °C (Bharti et al. 2015).

All the methods employed to characterize the supported **1** indicate a certain kind of interaction between the mesoporous particles and the complex. Vibrational features and thermal stability of the supported complex demonstrated that the silica support has a stabilizing effect on the complex. Moreover, we found a reduction in the surface areas after supporting **1** which would imply that the complex is internalized in the pores. However, this drop in the isotherm can be explained by the presence of a solid material (the copper complex here) with a small specific surface area (see for instance Arnal et al. 2006). Thus, instead of locating in the mesopores, most of the complex seems to locate on the outer surface of mesoporous silica spheres. Backfilling is a simple strategy for introducing active molecules into the empty pores of mesostructured silica, just by treating a material to a solution or vapor containing the active molecules and allowing it to diffuse into the material (Rytönen et al. 2012). However, in our case we could not demonstrate that the complex has entered the pores of silica, although it is supported in some way.

On the other hand, we observed that the release of **1** from the mesoporous particles is load dependent and the amount released correlates with the concentrations used for the loading. Similar results were obtained with the release of toremifene citrate from silica xerogel carrier material (Ahola et al. 2000), as well as vancomycin from silica sol–gel (Radin et al. 2001).

Cell viability was also determined in human osteosarcoma and normal phenotype osteoblast cell lines for supported and dissolved **1** at both concentrations. Our findings showed a beneficial effect in inhibiting the growth of osteosarcoma cells when the complex is delivered from the silica spheres. On the other hand, the effect of supported **1** on normal phenotype mouse calvaria cells was similar than the direct exposure of **1**. Our findings agree with similar systems. Loading curcumin on mesoporous silica nanoparticles significantly improved inhibition of breast cancer proliferation (Wang et al. 2016). Moreover, inhibition of superficial bladder cancer significantly improved when doxorubicin was supported on mesoporous silica nanoparticles (Zhang et al. 2014). However, releasing **1** exclusively from within the mesopores might further reduce tumor cell viability based on the ability of mesoporous spheres to cross cell walls and deploy its cargo within the cell. This, however, will require a further study to determine the experimental conditions required to selectively filling the mesopores with **1**.

Conclusion

Our *in vitro* study successfully shows that **1** induced cyto- and genotoxic effects. It is also well established that **1** outperformed either constituent ($[\text{Cu}(\text{H}_2\text{O})_6]^{2+}$, smz, and bipy) and **2** in reducing tumor cell viability, and that supporting **1** on mesoporous silica spheres improves it—even though **1** did not exclusively locate within mesopores of silica spheres. Future work aiming at exclusively filling of mesopores with **1** may determine if tumor cells turn unviable even more without any reduction of viability in normal cells, which will make **1** an interesting candidate for further *in vivo* studies.

Acknowledgements The work was supported by UNLP (11X/690), CONICET (PIP 0105), and ANPCyT (PICT 2014-2223, PICT 2014-2583 and PICT 2016-0508) from Argentina.

Compliance with ethical standards

Conflict of interest The authors declare that they have no conflict of interest.

References

- Ahola M, Kortesus P, Kangasniemi I, Kiesvaara J, Yli-Urpo A (2000) Silica xerogel carrier material for controlled release of toremifene citrate. *Int J Pharm* 195(1–2):219–227
- Anderson RJ, Groundwater PW, Todd A, Worsley AJ (2012) Sulfonamide antibacterial agents. Wiley, Chichester, pp 103–126
- Arjmand F, Muddassir M (2011) A mechanistic approach for the DNA binding of chiral enantiomeric L- and D-tryptophan-derived metal complexes of 1,2-DACH: cleavage and antitumor activity. *Chirality* 23(3):250–259
- Arnal PM, Schüth F, Kleitz F (2006) A versatile method for the production of monodisperse spherical particles and hollow particles: templating from binary core-shell structures. *Chem Commun* 11:1203–1205
- Azqueta A, Collins AR (2013) The essential comet assay: a comprehensive guide to measuring DNA damage and repair. *Arch Toxicol* 87(6):949–968
- Becco L, García-Ramos JC, Azuara LR, Gambino D, Garat B (2014) Analysis of the DNA interaction of copper compounds belonging to the Casiopeínas[®] antitumoral series. *Biol Trace Elem Res* 161(2):210–215
- Bharti C, Nagaich U, Pal AK, Gulati N (2015) Mesoporous silica nanoparticles in target drug delivery system: a review. *Int J Pharm Investig* 5(3):124–133
- Boulsourani Z, Katsamakos S, Geromichalos GD, Psycharis V, Raptopoulou CP, Hadjipavlou-Litina D et al (2017) Synthesis, structure elucidation and biological evaluation of triple bridged dinuclear copper(II) complexes as anticancer and antioxidant/anti-inflammatory agents. *Mater Sci Eng, C* 76:1026–1040
- Buchtík R, Trávníček Z, Vančo J, Herchel R, Dvořák Z (2011) Synthesis, characterization, DNA interaction and cleavage, and in vitro cytotoxicity of copper(ii) mixed-ligand complexes with 2-phenyl-3-hydroxy-4(1H)-quinolinone. *Dalton Trans* 40(37):9404
- Buchtík R, Trávníček Z, Vančo J (2012) In vitro cytotoxicity, DNA cleavage and SOD-mimic activity of copper(II) mixed-ligand quinolinato complexes. *J Inorg Biochem* 116:163–171
- Cadavid-Vargas J, Leon I, Etcheverry S, Santi E, Torre M, Di Virgilio A (2017) Copper(II) complexes with saccharinate and glutamine as antitumor agents: cytoand genotoxicity in human osteosarcoma cells. *Anticancer Agents Med Chem* 17(3):424–433
- Carter MT, Rodriguez M, Bard AJ (1989) Voltammetric studies of the interaction of metal chelates with DNA. 2. Tris-chelated complexes of cobalt(III) and iron(II) with 1,10-phenanthroline and 2,2'-bipyridine. *J Am Chem Soc* 111(24):8901–8911
- Chang D, Gao Y, Wang L, Liu G, Chen Y, Wang T et al (2016) Polydopamine-based surface modification of mesoporous silica nanoparticles as pH-sensitive drug delivery vehicles for cancer therapy. *J Colloid Interface Sci* 463:279–287
- Chen X, Tang L-J, Sun Y-N, Qiu P-H, Liang G (2010) Syntheses, characterization and antitumor activities of transition metal complexes with isoflavone. *J Inorg Biochem* 104(4):379–384
- Cusumano M, Di Pietro ML, Giannetto A, Vainiglia PA (2005) The intercalation to DNA of bipyridyl complexes of platinum(II) with thioureas. *J Inorg Biochem* 99(2):560–565
- Czekanska EM, Stoddart MJ, Richards RG, Hayes JS (2012) In search of an osteoblast cell model for in vitro research. *Eur Cells Mater* 24:1–17. <https://doi.org/10.22203/ecm.v024a01>
- Dong A, Ren N, Yang W, Wang Y, Zhang Y, Wang D et al (2003) Preparation of hollow zeolite spheres and three-dimensionally ordered macroporous zeolite monoliths with functionalized interiors. *Adv Funct Mater* 13(12):943–948
- Duff B, Reddy Thangella V, Creaven BS, Walsh M, Egan DA (2012) Anti-cancer activity and mutagenic potential of novel copper(II) quinolinone Schiff base complexes in hepatocarcinoma cells. *Eur J Pharmacol* 689(1–3):45–55
- Fenech M (2000) The in vitro micronucleus technique. *Mutat Res Mol Mech Mutagen* 455(1–2):81–95
- Ferrari MB, Bisceglie F, Pelosi G, Tarasconi P, Albertini R, Dall'Aglio PP et al (2004) Synthesis, characterization and biological activity of copper complexes with pyridoxal thiosemicarbazone derivatives. X-ray crystal structure of three dimeric complexes. *J Inorg Biochem* 98(2):301–312
- Filho JCC, Sarria ALF, Becceneri AB, Fuzer AM, Batalhão JR, da Silva CMP et al (2014) Copper (II) and 2,2'-bipyridine complexation improves chemopreventive effects of naringenin against breast tumor cells. *PLoS ONE* 9(9):e107058
- Finn NA, Kemp ML (2012) Pro-oxidant and antioxidant effects of N-acetylcysteine regulate doxorubicin-induced NF-kappa B activity in leukemic cells. *Mol BioSyst* 8(2):650–662
- Galindo-Murillo R, Hernandez-Lima J, González-Rendón M, Cortés-Guzmán F, Ruíz-Azuara L, Moreno-Esparza R (2011) π -Stacking between Casiopeínas[®] and DNA bases. *Phys Chem Chem Phys* 13(32):14510
- Galindo-Murillo R, García-Ramos JC, Ruiz-Azuara L, Cheatham TE, Cortés-Guzmán F, Cortés-Guzmán F (2015) Intercalation processes of copper complexes in DNA. *Nucleic Acids Res* 43(11):5364–5376
- Gaur R, Choubey DK, Usman M, Ward BD, Roy JK, Mishra L (2017) Synthesis, structures, nuclease activity, cytotoxicity, DFT and molecular docking studies of two nitrate bridged homodinuclear (Cu-Cu, Zn-Zn) complexes containing 2,2'-bipyridine and a chalcone derivative. *J Photochem Photobiol B Biol* 173:650–660
- Gutiérrez L, Alzuet G, Borrás J, Castiñeiras A, Rodríguez-Fortea A, Ruiz E (2001) Copper(II) complexes with 4-amino-N-[4,6-dimethyl-2-pyrimidinyl]benzenesulfonamide. Synthesis, crystal structure, magnetic properties, EPR, and theoretical studies of a novel mixed μ -carboxylato NCN-bridged dinuclear copper compound. *Inorg Chem* 40(13):3089–3096
- Hossain GMG, Amoroso AJ, Banu A, Malik KMA (2007) Syntheses and characterisation of mercury complexes of

- sulfadiazine, sulfamerazine and sulfamethazine. *Polyhedron* 26(5):967–974
- Karlsson H, Fryknäs M, Strese S, Gullbo J, Westman G, Bremberg U et al (2017) Mechanistic characterization of a copper containing thiosemicarbazone with potent antitumor activity. *Oncotarget* 8(18):30217–30234
- León IE, Cadavid-Vargas JF, Di Virgilio AL, Etcheverry S (2016) Vanadium, ruthenium and copper compounds: a new class of non-platinum Metallo drugs with anticancer activity. *Curr Med Chem* 12(2):309–316
- Lobana TS, Indoria S, Jassal AK, Kaur H, Arora DS, Jasinski JP (2014) Synthesis, structures, spectroscopy and antimicrobial properties of complexes of copper(II) with salicylaldehyde N-substituted thiosemicarbazones and 2,2'-bipyridine or 1,10-phenanthroline. *Eur J Med Chem* 76:145–154
- Lu J, Liong M, Zink JI, Tamanoi F (2007) Mesoporous silica nanoparticles as a delivery system for hydrophobic. *Anticancer Drugs* 3(8):1341–1346
- Mai Z, Chen J, Hu Y, Liu F, Fu B, Zhang H et al (2017) Novel functional mesoporous silica nanoparticles loaded with Vitamin E acetate as smart platforms for pH responsive delivery with high bioactivity. *J Colloid Interface Sci* 508:184–195
- Mansour AM, Mohamed RR (2015) Sulfamethazine copper(ii) complexes as antimicrobial thermal stabilizers and costabilizers for rigid PVC: spectroscopic, thermal, and DFT studies. *RSC Adv* 5(7):5415–5423
- Martínez-Carmona M, Lozano D, Colilla M, Vallet-Regí M (2016) Selective topotecan delivery to cancer cells by targeted pH-sensitive mesoporous silica nanoparticles. *RSC Adv* 6(56):50923–50932
- Mosmann T (1983) Rapid colorimetric assay for cellular growth and survival: application to proliferation and cytotoxicity assays. *J Immunol* 65(1–2):55–63
- Nordberg J, Arnér ESJ (2001) Reactive oxygen species, antioxidants, and the mammalian thioredoxin system. *Free Radic Biol Med* 31(11):1287–1312
- Oliveri V, Lanza V, Milardi D, Viale M, Maric I, Sgarlata C et al (2017) Amino- and chloro-8-hydroxyquinolines and their copper complexes as proteasome inhibitors and antiproliferative agents. *Metallomics* 9(10):1439–1446
- Öztürk F, Bulut İ, Bulut A (2015) Structural, spectroscopic, magnetic and electrochemical studies of monomer N-substituted-sulfanilamide copper (II) complex with 2,2'-bipyridine. *Spectrochim Acta, Part A* 138:891–899
- Pautke C, Schieker M, Tischer T, Kolk A, Neth P, Mutschler W, Milz S (2004) Characterization of osteosarcoma cell lines MG-63, Saos-2 and U-2 OS in comparison to human osteoblasts. *Anticancer Res* 24:3743–3748
- Piotrowska-Kirschling A, Drzeżdżon J, Kloska A, Wyrzykowski D, Chmurzyński L, Jacewicz D (2018) Antioxidant and cytoprotective activity of oxydiacetate complexes of cobalt(II) and nickel(II) with 1,10-phenanthroline and 2,2'-bipyridine. *Biol Trace Elem Res* 185(1):244–251
- Radin S, Ducheyne P, Kamplain T, Tan BH (2001) Silica sol-gel for the controlled release of antibiotics. I. Synthesis, characterization, and in vitro release. *J Biomed Mater Res* 57(2):313–320
- Royall JA, Ischiropoulos H (1993) Evaluation of 2',7'-Dichlorofluorescein and dihydrorhodamine 123 as fluorescent probes for intracellular H₂O₂ in cultured endothelial cells. *Arch Biochem Biophys* 302(2):348–355
- Rytkönen J, Miettinen R, Kaasalainen M, Lehto V-P, Salonen J, Närvänen A (2012) Functionalization of mesoporous silicon nanoparticles for targeting and bioimaging purposes. *J Nanomater* 2012:1–9
- Santini C, Pellei M, Gandin V, Porchia M, Tisato F, Marzano C (2014) Advances in copper complexes as anticancer agents. *Chem Rev* 114(1):815–862
- Seng H-L, Wang W-S, Kong S-M, Alan Ong H-K, Win Y-F, Abd Raja, Rahman RNZ et al (2012) Biological and cytoselective anticancer properties of copper(II)-polypyridyl complexes modulated by auxiliary methylated glycine ligand. *Biomaterials* 25(5):1061–1081
- Serment-Guerrero J, Cano-Sanchez P, Reyes-Perez E, Velazquez-Garcia F, Bravo-Gomez ME, Ruiz-Azuara L (2011) Genotoxicity of the copper antineoplastic coordination complexes casiopeinas. *Toxicol* 25(7):1376–1384
- Singh NP, McCoy MT, Tice RR, Schneider EL (1988) A simple technique for quantitation of low levels of DNA damage in individual cells. *Exp Cell Res* 175(1):184–191
- Stopper H, Müller SO (1997) Micronuclei as a biological endpoint for genotoxicity: a minireview. *Toxicol Vitro* 11(5):661–667
- Tommasino J-B, Renaud FNR, Luneau D, Pilet G (2011) Multifunctional complexes combining antiseptic copper(II) with antibiotic sulfonamide ligands: structural, redox and antibacterial study. *Polyhedron* 30(10):1663–1670
- Wang J, Wang Y, Liu Q, Yang L, Zhu R, Yu C et al (2016) Rational design of multifunctional dendritic mesoporous silica nanoparticles to load curcumin and enhance efficacy for breast cancer therapy. *ACS Appl Mater Interfaces* 8(40):26511–26523
- Xu F, Ding L, Tao W, Yang X, Qian H, Yao R (2016) Mesoporous-silica-coated upconversion nanoparticles loaded with vitamin B12 for near-infrared-light mediated photodynamic therapy. *Mater Lett* 167:205–208
- Zhang H, Thomas R, Oupicky D, Peng F (2007) Synthesis and characterization of new copper thiosemicarbazone complexes with an ONNS quadridentate system: cell growth inhibition, S-phase cell cycle arrest and proapoptotic activities on cisplatin-resistant neuroblastoma cells. *J Biol Inorg Chem* 13(1):47–55
- Zhang Q, Neoh KG, Xu L, Lu S, Kang ET, Mahendran R et al (2014) Functionalized mesoporous silica nanoparticles with mucoadhesive and sustained drug release properties for potential bladder cancer therapy. *Langmuir* 30(21):6151–6161